FLEXURAL WAVES GENERATED BY COHERENT SOURCES IN ARCTIC SEA ICE

D. Benjamin Reeder Naval Postgraduate School, Monterey, California, USA
John E. Joseph Naval Postgraduate School, Monterey, California, USA
Colleen M. Wilmington Naval Postgraduate School, Monterey, California, USA
Taylor B. Hudson Naval Postgraduate School, Monterey, California, USA

1 INTRODUCTION

Arctic climate is important on global and regional scales, influencing global temperatures, global sea level, and commercial and native coastal community activities. The Arctic energy budget is controlled by atmospheric temperatures, cloud cover, wind patterns, freshwater discharge, oceanic forcing and sea ice cover. Of particular importance, sea ice cover buffers air-sea heat flux and modulates solar radiation absorption. The Arctic environment has been experiencing changes in recent decades: (a) average increases in atmospheric temperatures exceed those of the rest of the globe by a factor of two;[1,2,3] (b) the summer sea ice area coverage is 40% lower;[4,5,6] and (c) average sea ice thickness has decreased.[4,7] While the Arctic continues to be ice-covered for a vast majority of the year, an increasingly larger fraction of the winter sea ice is first-year ice. Given these recent changes to the Arctic environment, new observations and modeling are required in order to understand the relative contributions of these environmental parameters and to better predict Arctic climate. To that end, work in the 1980s demonstrated that mechanical properties of Arctic sea ice can be inferred by observation of the speeds of compressional, shear and flexural waves generated through in-ice conversion of impulsive energy.[8,9] The work presented here (a) advances the work from the 1980s and 1990s by making use of coherent sources with which broadband signals can be generated to replace the manually-generated signals, leveraging processing gain and improving temporal resolution via matched filter; and (b) demonstrates the potential for remote, autonomous monitoring of sea ice mechanical properties.

2 ACOUSTIC WAVES IN ARCTIC SEA ICE

Arctic ocean circulation models are informed by sea ice models, the primary parameter of which is ice thickness. The high degree of uncertainty in the two primary means of sea ice thickness estimation--passive microwave and altimetry--is enhanced by snow cover.[10] *In situ* methods of ice property inference were studied near the end of the Cold War in the 1980's and 1990's.[8,9] These methods relied on the elastic properties of the ice sheet: the compressional, shear and flexural wave energies have different wave speeds.[11,12,13,14] Mechanical properties of the ice were inferred through a series of equations relating the observed wave speeds to sea ice properties; specifically, the bulk modulus of elasticity, ice density, Poisson's ratio and ice thickness.[8,15] More recently, it was discovered that the mere act of walking on the ice sheet generates resonances in the ice, the frequencies of which correlate to ice thickness.[16] These investigations relied upon impulsive or near-impulsive sources of sound (e.g., explosive sources in the water, hammer/ball drops and footsteps) applied directly to the ice. Rather than relying on anthropogenically-induced signals, vibrational energy generated by natural sources (e.g., seismic signals, ice cracking and ridging, ice floes rubbing at the edges[17,18,19]) has been recently exploited for passive ice property inference.[20,21]

The use of active sources such as lead ball drops on the ice offers advantages in terms of a somewhat controlled, broadband source signal (depending on weight and height of release) and known timing, while possessing inherent risk and expense (humans on floating ice in a hazardous environment). The use of passive sources offers less risk, but less control and more signal processing investment. A new alternative approach to ice property inference presented here consists of using electrically-driven coherent sources to probe the ice with broadband signals. This approach provides a number of advantages over impulses generated by ball drops and natural sources: (a) control of signal

spectral content, (b) expanded spectral content (higher source levels at higher frequencies), (c) significant processing gain, (d) increased temporal resolution, and (e) the potential for remote deployment and operation.

This new approach requires sources and receivers designed to excite and observe signals in elastic substrates rather than those designed for in-water use. The sources used in this work are "tactile sound transducers" (TST) and the receivers are "cryophones", details of which are presented in the next section.

3 DATA COLLECTION

In March 2024, an acoustics field experiment was conducted during Ice Camp Whale, established and maintained by the U.S. Navy Arctic Submarine Laboratory. Located approximately 200 nm NNE of Prudhoe Bay, Alaska in the Beaufort Sea in 12,000 ft. of water, the ice camp experienced light and variable winds during the acoustic data collection period. The ice floe consisted of both first-year and multi-year ice: the ice camp itself was built on multi-year ice, while the acoustic tests were conducted on first-year ice that was approximately 1.2 m thick. Figure 1 shows the instrument laydown pattern with separation distances anchored at the Vertical Line Array (VLA) of four hydrophones in the water column (black), three different TSTs (red), four single-channel (S#) and three triaxial (T#) cryophones (black) and an eight-channel microphone array (green). The TSTs and cryophones were frozen into the top two inches of ice to ensure good transfer of vibrational energy between the ice and the instrument. The microphone array was suspended 10-15 cm above the ice.

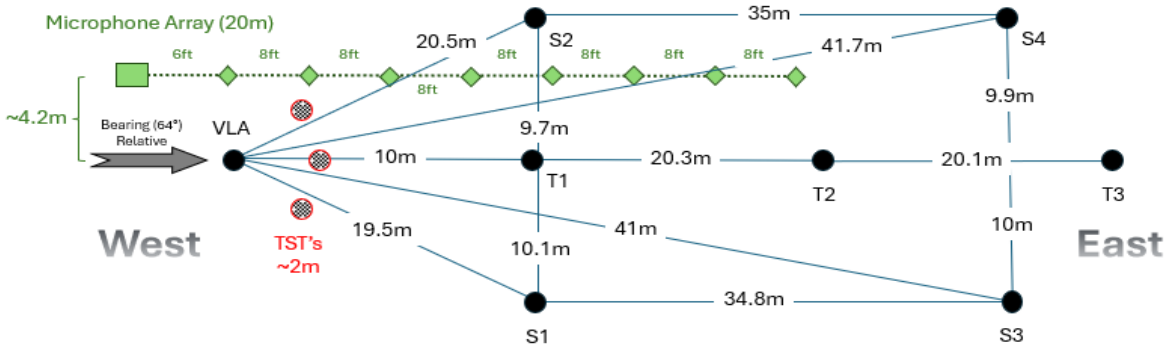

Figure 1. Instrument laydown pattern in first-year sea ice in the Beaufort Sea in March 2024, consisting of a Vertical Line Array (VLA, black) of hydrophones in the water, Tactical Sound Transducers (TST, red) and cryophones (S# and T#, black) frozen into the ice, and an 8-channel microphone array suspended 10-15 cm above the ice (green).

There were three different TSTs designed to drive vibrations in elastic substrates: SolidDrive SD1, ClarkSynthesis AW439 and the Buttkicker CT; each has its own nominal spectral response band (60-15,000 Hz, 5-17,000 Hz, 5-200 Hz). The TSTs were driven by battery-powered amplifiers, and the signals were provided in .wav files by Apple Nano audio players.

The cryophones consisted of accelerometers (PCB Piezotronics, Models 306M133 and 393B05), pre-amp signal conditioners (PCB Piezotronics, Model 485B36) and single-channel, AudioMoth digital recorders,[22] installed inside 4-inch diameter, 8'-15" tall Blue Robotics acrylic cylinders with aluminum endplates.

A series of linear frequency modulated (LFM) signals with different bands and pulselengths were transmitted by the TSTs, in order to explore the signal space for optimal in-ice transmission characteristics. The bands spanned frequencies of 10 Hz to 10 kHz, and the pulselengths ranged

from 0.01 seconds to 5 seconds. Each signal was separated by a 6-second inter-pulse period, to minimize the chance of signal overlap by reflections from the seabed. The entire 1.25-hour long series of signals was played in the evening hours during periods of minimal camp activity to minimize corrupting background noise in the signal received by the cryophones.

4 ANALYSIS

The use of coherent broadband LFM signals generated by electrically-driven sources facilitates the use of matched filter signal processing (MFP). The MFP provides significant processing gain, increases temporal resolution, and acts as an out-of-band and in-band noise filter. The results below are derived from the data collected very recently, and thus, are considered preliminary in nature. The analysis presented here is limited to signals transmitted by the SolidDrive TST and received by single-channel vertically-oriented cryophones S2 and S4 on March 7, 2024.

Figure 2 is a plot of matched filter output (MFO) relative amplitude vs. time (hh:mm:ss.s Z) of signals received at S2 (blue) and S4 (red) after being transmitted by TST SD1. The transmitted signal in this case was a 2-second long, 10-500 Hz LFM. The MFO peaks are separated in time by 37 msec and differ in magnitude by a factor of 3.5. Each reception consists of a peak followed by a low-frequency tail below 100 Hz. The late-arriving low-frequency tail is due to the dispersion of vertically-oriented flexural waves whose phase speeds are proportional to frequency.

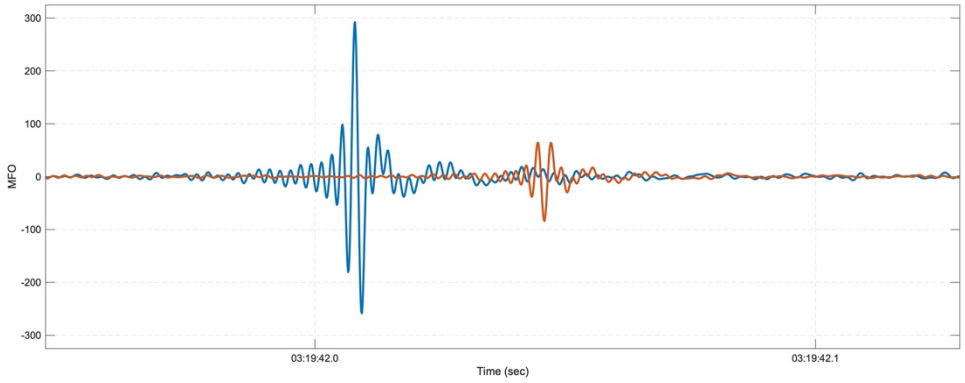

Figure 2. Matched filter output (MFO) relative amplitude vs. time (hh:mm:ss.s Z) of signals received at S2 (blue) and S4 (red).

Figure 3 presents the spatial, temporal and spectral structure of relative energy level (dB) of the arrival in Figure 2 at S2 as a function of relative arrival time (sec) on the vertical axis and frequency (Hz) on the horizontal axis. The earliest-arriving energy is in the 100-500 Hz band while the low-frequency tail occurs below 100 Hz. No dispersion is observed above 100 Hz because the S2-S4 separation distance was only 21.2 m in the cryophone laydown geometry; the higher-speed frequencies in the signal had insufficient range over which to separate in time and space. No dispersion is observed below 45 Hz because the SD1 TST, with a nominal frequency response band of 60-15,000 Hz, transmitted insufficient energy below 45 Hz. The maximum signal spectral level observed at S2 (black) and S4 (red) in each frequency bin and a 4th degree polynomial fit are plotted as circles and lines, respectively. Each arrival is approximated by a fifth-degree polynomial fit, in order to extend the results to lower frequencies and better illustrate the low-frequency tail. These fits aid the estimation of the time difference of the arrivals and thus, flexural wave phase speed as a function of frequency between 15 Hz and 100 Hz.

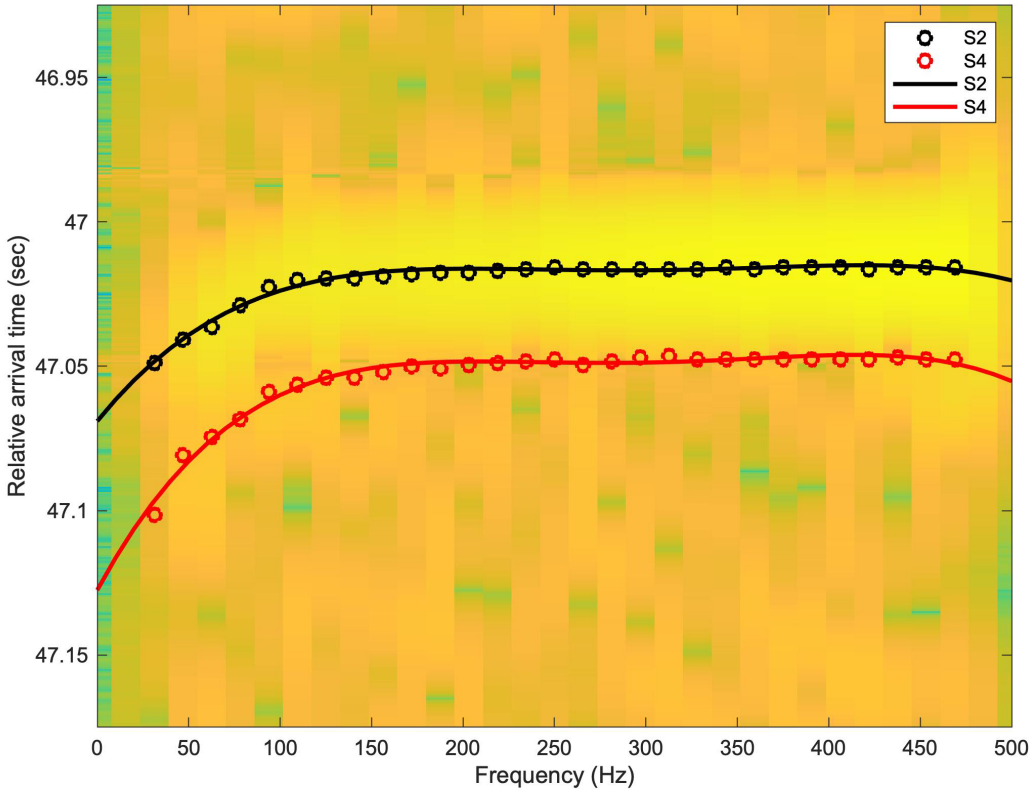

Figure 3. Relative energy level (dB) of the arrival in Figure 2 at S2 as a function of relative arrival time (sec) on the vertical axis and frequency (Hz) on the horizontal axis; maximum signal spectral level observed at S2 (black) and S4 (red) in each frequency bin (circles) and a 4th degree polynomial fit (lines).

Figure 4 displays flexural wave phase speed (m/s) as a function of frequency (Hz) of this particular observed set of arrivals (circles) and the modeled phase speed (line) of 1.2 m thick ice using nominal values of mechanical properties (i.e., E = 7.2 x 10^9 Pa, ρ_{ice} = 910 kg/m^3, ρ_{water} = 1000 kg/m^3, μ = 0.33, c_{water} = 1440 m/s, g = 9.8 m/s^2).[8,15] The agreement is good at 60 Hz, but the model under-predicts the observed phase speed at lower frequencies and over-predicts the observed phase speed at higher frequencies. There are at least two explanations for this disagreement: (1) the nominal values of mechanical ice properties used here are based on work done in the Beaufort Sea in the 1980's, which indicates that the properties of the ice may be different now than 40 years ago; and (2) while some dispersion is observable in Figure 3, the current 21.2 m separation distance between S2 and S4 is inadequate to allow sufficient time and space for signal dispersion to be properly observed.

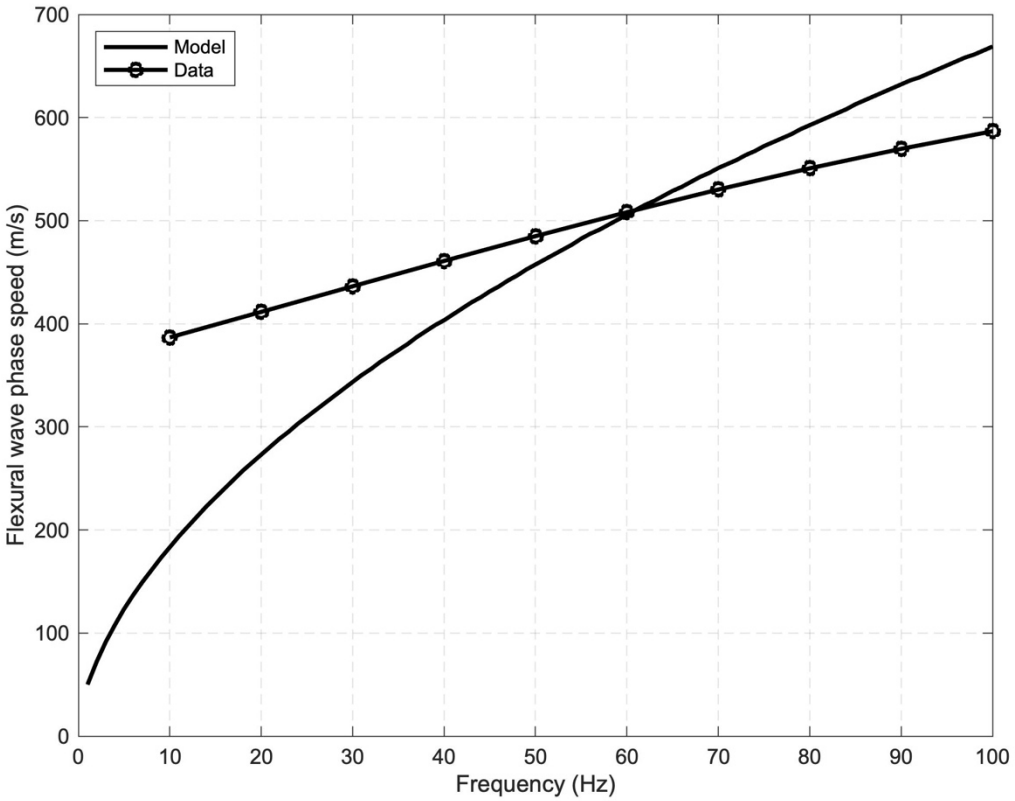

Figure 4. Flexural wave phase speed (m/s) as a function of frequency (Hz) of the observed set of arrivals in Figure 3 (circles) and the modeled phase speed (line) of 1.2 m thick ice using nominal values of mechanical properties.

5 CONCLUSION

An acoustics field experiment was conducted during Ice Camp Whale in March 2024 on an ice floe in the Beaufort Sea, 200 nm NNE of Prudhoe Bay, Alaska, USA. Instruments were frozen into the top 2 inches of 1.2 m thick first-year ice to investigate the in-ice propagation of compressional, shear and flexural waves generated by electrically-driven TSTs. This particular paper presents initial analysis on a small subset of the data: 2-second long, 10-500 Hz broadband LFM signals. The signals received by cryophones were matched filtered to increase signal-to-noise ratio and temporal resolution. The MFO structure contains low-frequency tails below 100 Hz resulting from frequency-dependent wave speed dispersion. The frequency-dependent time difference of arrivals at two cryophones were used to estimate flexural wave phase speed of 400-600 m/s between 10 and 100 Hz. These initial results are approximately consistent with work published in the 1980's and 1990's[8,9] and with modeled flexural wave phase speed[8,15]. Further analysis continues on the entire dataset.

Significantly, this work demonstrates that (1) flexural wave phase speed dispersion was observed, after having been (2) generated by a coherent, ice-bound electrically-driven source. This approach to sea ice property inference provides a number of advantages over impulses generated by ball drops and natural sources, including control of and expanded spectral content, significant processing gain and temporal resolution, and the potential for remote, autonomous, persistent monitoring of ice properties.

6 REFERENCES

1. Serreze, M. C., A.P. Barrett, J.C. Stroeve, D.N. Kindig and M.M. Holland (2009). “The emergence of surface-based Arctic amplification”, *Cryosphere*, 3, 11–19.

2. Screen, J. A., and I. Simmonds (2010). “The central role of diminishing sea ice in recent Arctic temperature amplification”, *Nature*, 464, 1334–1337.

3. Osborne, E., J. Richter-Menge and M. Jeffries (2018). “Arctic Report Card 2018”, https://www.arctic.noaa.gov/Report-Card (Last viewed February 27, 2024).

4. Stroeve, J., and W. Maslowski (2007). “Arctic sea ice variability during the last half century”, in *Climate Variability and Extremes During the Past 100 Years*, edited by S. Bronnimann, J. Luterbacher, T. Ewen, H. F. Diaz, R. S. Stolarski and U. Neu, Springer, Amsterdam, pp. 143–154.

5. Stroeve, J.C., M.C. Serreze, M.M. Holland, J.E. Kay, J. Maslanik and A.P. Barrett (2012). “The Arctic’s rapidly shrinking sea ice cover: A research synthesis”, *Clim. Change*, 110, 1005–1027.

6. Maslowski, W., J.C. Kinney, M. Higgins and A. Roberts (2012). “The future of Arctic sea ice”, *Annu. Rev. Earth Planet. Sci.*, 40, 625–654.

7. Kwok, R., and N. Untersteiner (2011). “The thinning of Arctic sea ice”, *Phys. Today*, 64(4), 36–41.

8. Stein, P.J., S.E. Euerle and J.C. Parinella (1998). “Inversion of pack ice elastic wave data to obtain ice physical properties”, *J. Geophys. Res*., 103(C10), 21783–21793, https://doi.org/10.1029/98JC01269.

9. Xie, Y. and D.M. Farmer (1994). “Seismo-acoustic sensing of sea ice properties”, *J. Geophys. Res*., 99(C4), 7771–7786, https://doi.org/10.1029/93JC03483.

10. Xiao, F., F. Li, S. Zhang, J. Li, T. Geng and Y. Xuan (2020). “Estimating Arctic Sea ice thickness with CryoSat-2 altimetry data using the least squares adjustment method”, *Sensors*, 20(24), 7011.

11. Ewing, M., A.P. Crary and A.M. Thorne (1934). “Propagation of elastic waves in ice. Part I”, *Physics*, 5, 165–168.

12. Ewing, M., A.P. Crary and A.M. Thorne (1934). “Propagation of elastic waves in ice. Part II”, *Physics*, 5, 181–184.

13. Press, F., and W.M. Ewing (1951). “Propagation of elastic waves in a floating ice sheet”, *Eos Trans. AGU*, 32, 673–678.

14. Moreau, L., C. Lachaud, R. Thry, M.V. Predoi, D. Marsan, J. Weiss and M. Montagnat (2017). "Monitoring ice thickness and elastic properties from the measurement of leaky guided waves: A laboratory experiment", *J. Ac. Soc. Am*., 142(5), 2873–2880, https://doi.org/10.1121/1.5009933.

15. Cremer, L., M. Heckl and E.E. Ungar, *Structure-Born Sound*, Springer-Verlag, New York, 1973.

16. Reeder, D. Benjamin, J.E. Joseph, A. Hill and K. Ainslie (2022). “Walking on snow-covered Arctic ice to infer ice thickness”, *J. Acoust. Soc. Am*., 152(6), 3809–3818.

17. Farmer, D., and Y. Xie (1989). “The sound generated by propagating cracks in sea ice”, *J. Acoust. Soc. Am.*, 85, 1489–1500.

18. Xie, Y., and D.M. Farmer (1992). “The sound of ice break-up and floe interaction”, *J. Acoust. Soc. Am.*, 91(3), 1423–1428.

19. Ye, Z. (2004). “Sound generated by rubbing objects”, *Phys. Lett. A*, 327, 91–94.

20. Moreau, L., P.Boué, A. Serripierri, J. Weiss, D. Hollis, I. Pondaven, B. Vial, S. Garambois, É. Larose, A. Helmstetter, L. Stehly, G. Hillers and O. Gilbert (2020). “Sea ice thickness and elastic properties from the analysis of multimodal guided wave propagation measured with a passive seismic array”, *J. Geophys. Res. Oceans*, 125, e2019JC015709, doi.org/10.1029/2019JC015709.

21. Reeder, D. Benjamin, J.E. Joseph and S.K. Wheeler (2024), "Passive sea ice thickness inference using cryophones", *J. Acoust. Soc. Am. EL*, 4(3), 1-7, 030801, doi.org/10.1121/10.0025241.

22. Hill, A.P., P. Prince, J.L. Snaddon, C.P. Doncaster and A. Rogers (2019). "AudioMoth: A low-cost acoustic device for monitoring biodiversity and the environment", *HardwareX*, 6, 1-20.